J. Fluid Mech. (1992), *vol.* 244, *pp.* 187–200

On the shape of a two-dimensional bubble in uniform motion

By P. N. SHANKAR

Computational and Theoretical Fluid Dynamics Division, National Aeronautical Laboratory, Bangalore 560 017, India

(Received 14 October 1991 and in revised form 23 April 1992)

Consider a two-dimensional bubble moving with speed U through an unbounded, inviscid fluid. Let all lengths be normalized by $T/\rho U^2$ where T is the surface tension. Then the shape of the bubble depends on a single parameter $\Gamma = 2\Delta p/\rho U^2 - 1$, where $\Delta p = p_b - p_\infty$ is the difference between the bubble pressure and the ambient pressure. We obtain solutions for the bubble shape over the whole range of Γ-values that are physically relevant. The formulation involves a mapping from an auxiliary circle plane ζ where the flow field is known. The problem then reduces to solving an infinite set of nonlinear algebraic equations for the coefficients in the mapping function.

To a first approximation, when $\Gamma \to \infty$, the bubble takes an elliptical shape of aspect ratio $(1+\frac{2}{3}\Gamma^{-1})/(1-\frac{2}{3}\Gamma^{-1})$ flattened in the flow direction. The solution correct to order Γ^{-5} is then obtained which is fairly accurate for Γ as low as 2. When $\Gamma = 0$ the exact, nonlinear solution for the bubble shape is given by $x = \frac{1}{3}(\frac{1}{3}\cos\phi - \frac{1}{27}\cos 3\phi)$, $y = \frac{1}{3}(\frac{5}{3}\sin\phi + \frac{1}{27}\sin 3\phi)$. We can then obtain a perturbation solution for $\Gamma \to 0$ correct to order Γ^6. This solution, useful in the range $0.75 > \Gamma > -0.4537$, even gives reasonable descriptions of non-convex bubble shapes for $\Gamma < 0$ down to the pinch-off limit Γ^* when the bubble ceases to be simply connected. It is remarkable that a simple analytical representation correct to order Γ^2 analytically yields a value for Γ^* of -0.4548, i.e. within 0.3% of the correct value; naturally, the higher-order approximations are even more accurate. While the present results eliminate the need for direct numerical computations over most of the range of Γ, such results, too, are presented. Finally, the dependence of the bubble geometrical parameters, Weber number and added mass on Γ is determined.

1. Introduction

The question we wish to address is the following: what shape does a two-dimensional bubble take when it moves at constant speed through an inviscid, incompressible fluid? Naturally, the shape will depend on U the speed, $\mathscr{A}$ the cross-sectional area of the bubble, $(p_b - p_\infty)$ the difference between the uniform bubble pressure and the pressure at infinity, ρ the density of the fluid and the surface tension T. The dependence on all these parameters can easily be shown to reduce to that on a single non-dimensional parameter $\Gamma = 2(p_b - p_\infty)/\rho U^2 - 1$, a dimensionless pressure parameter related to the cavitation number.

The above problem can arise in a physical context as follows. If a bubble is formed in a fluid of low viscosity and begins to move rapidly, the velocity can become uniform if the small drag force on the bubble exactly balances the external force on it, usually buoyancy. If the Reynolds number is sufficiently high, as it often is, the viscous effects can be shown to be confined to a narrow boundary layer on the surface

of the bubble (Moore 1959, 1965). Under these circumstances, the shape of the steadily moving bubble will be determined principally by the inviscid flow field.

In the case of axisymmetric bubbles, Moore in the papers referred to above, assumed the bubbles to be oblate ellipsoids of revolution and approximately computed their geometrical parameters. Apart from estimating the shapes of the bubbles, Moore showed that there is a maximum value of the Weber number (≈ 3.74) above which no steady axisymmetric solution exists. A much more complete attack on the problem was made by Miksis, Vanden-Broeck & Keller (1981) who computed axisymmetric bubble shapes over the whole range from $\Gamma \to \infty$ to close to the lower limit for Γ (≈ -0.31), when the bubble becomes toroidal. By this direct numerical attack on the full nonlinear free boundary problem not only were the earlier conclusions confirmed but a number of new interesting features were also revealed. More recent work in the area include the promising general Hamiltonian formulation of Benjamin (1987), the unsteady calculations of Baker & Moore (1989) for the two-dimensional case and the computations of vortex ring bubbles by Lundgren & Mansour (1991). The latter two are again direct numerical calculations based on boundary-integral methods. Although Meiron (1989) is concerned mainly with the stability question, he presents some steady axisymmetric shapes based on a collocation method. Interestingly, though, he does not present any results, as Miksis *et al.* (1981) did, showing visible negative curvature near the stagnation point for negative Γ. This is probably due to the general difficulty of computing in this range of the parameter, irrespective of method.

A point to be noted is that most of the results currently available are numerical in nature with very few analytical results to hand. These few include Moore's (1959) approximate result for the bubble shape at small Weber numbers, and Walter & Davidson's (1962) small-time solution for the two-dimensional case in the absence of surface tension. The main aim of this paper is to obtain some analytical solutions that will hopefully clarify the nature of the problem in a way in which purely numerical solutions cannot. To this end we will consider the two-dimensional problem as the nonlinear free boundary problem is more likely to be tractable in this case. In what follows we will show how the powerful technique of conformal mapping can be manipulated to yield a number of interesting and valuable results. These include an accurate asymptotic solution for $\Gamma \to \infty$, the exact solution for $\Gamma = 0$ (earlier discovered by McLeod 1955) and a perturbation solution for $\Gamma \to 0$. Accurate numerical results are also presented for the whole range of Γ. Finally the dependence of the bubble perimeter and cross-sectional area and of the bubble Weber number and added mass on Γ is established.

2. Formulation

We shall work in a frame fixed to the bubble and consider uniform flow past it (see figure 1). Let the free-stream speed and pressure be U and p_∞ respectively; let p_b be the uniform pressure within the bubble. Assuming the fluid to be inviscid and the flow field to be irrotational we need only deal with a potential flow. The boundary conditions at infinity are obvious as is the condition that the bubble profile be a *stream*line. The only remaining condition is that at the bubble surface the pressure forces must be balanced by the forces due to surface tension, i.e.

$$\Delta p = p_b - p = T\hat{K} \tag{1}$$

where the pressure p refers to conditions in the fluid at the bubble surface and both

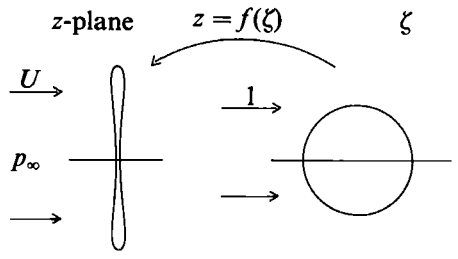

FIGURE 1. Steady, inviscid, incompressible flow past a bubble. The region exterior to the circle in the ζ-plane is mapped to the region exterior to the bubble in the physical plane.

p and the curvature $\hat{K}$ are obviously functions of position. Combining (1) with Bernoulli's equation we find

$$\frac{\hat{q}^2}{U^2} = \frac{T\hat{K}}{\frac{1}{2}\rho U^2} - \left\{\frac{\Delta p}{\frac{1}{2}\rho U^2} - 1\right\} \tag{2}$$

where $\hat{q}$ is the fluid speed on the bubble surface. All velocities are normalized by U; more subtle is the normalization of all lengths by the lengthscale $T/\frac{1}{2}\rho U^2$ as suggested by Miksis *et al.*, which means that all computations need depend on a single parameter Γ, $\Gamma = (p_b - p_\infty)/(\frac{1}{2}\rho U^2) - 1$ alone; the surface tension T only changes the lengthscale. Equation (2) then takes the simple form

$$q^2 = K - \Gamma, \tag{3}$$

where q and K are the non-dimensional fluid speed and bubble surface curvature respectively. Thus the problem reduces to finding a velocity potential and bubble shape such that, in addition to satisfying the conditions at infinity, the bubble profile is a streamline and (3) is satisfied on it. Obviously, like most free boundary problems, the problem is nonlinear and in general difficult.

Working in the plane, it is natural to seek a solution based on conformal mapping. We therefore consider uniform flow of unit speed past a circle of radius R in the ζ-plane (figure 1); the complex potential is given by

$$w(\zeta) = (\zeta + R^2/\zeta) \tag{4}$$

We now seek to map the exterior of the circle in ζ to the exterior of the bubble in the z-plane by choosing a general mapping function of the form

$$z = f(\zeta) = \zeta + \sum_{n=1}^{\infty} \frac{R^{n+1} a_n}{\zeta^n} \tag{5}$$

where the coefficients a_n and the radius R are to be determined. Note that the mapping goes into the identity as $\zeta \to \infty$. Symmetry about the $y = 0$ plane requires that the a_n be real. A little reflection shows that in a potential flow the bubble has also be symmetric about $x = 0$. Consequently the even a_n, i.e. ones of the form a_{2k}, have to vanish; thus we are left with R and the odd coefficients $a_1, a_3, a_5 \ldots$.

It will prove to be convenient to define the coefficients $\gamma_n = n a_n$ for $n = 1, 3, 5, \ldots$ and to work with the γ_n rather than the a_n. From (4) and (5) the fluid speed on the bubble surface defined by $z = f[\zeta = R\exp(\mathrm{i}\phi)]$ is given by

$$q^2 = \frac{|\mathrm{d}w/\mathrm{d}\zeta|^2}{|\mathrm{d}z/\mathrm{d}\zeta|^2} = \frac{2(1-\cos 2\phi)}{\left(1 + \sum_{n=1}^{\infty} \gamma_n^2\right) - \sum_{n=1}^{\infty} 2\gamma_n \cos(n+1)\phi + \sum_{n=2}^{\infty}\left(\sum_{k=1}^{\infty} 2\gamma_k \gamma_{k+n}\right)\cos n\phi} \tag{6}$$

Before computing the curvature we first note from (5) for later reference that the bubble coordinates are given by

$$x(\phi) = R\left(\cos\phi + \sum_{n=1}^{\infty} a_n \cos n\phi\right), \tag{7a}$$

$$y(\phi) = R\left(\sin\phi - \sum_{n=1}^{\infty} a_n \sin n\phi\right). \tag{7b}$$

The formula for the curvature K is

$$K = \frac{x'y'' - y'x''}{(x'^2 + y'^2)^{\frac{3}{2}}}, \tag{8}$$

where the primes refer to differentiation with respect to ϕ. From (7) and (8) it follows that the curvature is given explicitly by the formula

$$K = \frac{\left(1 - \sum_{k=1}^{\infty} k\gamma_k^2\right) + \sum_{n=1}^{\infty} (n-1)\gamma_n \cos(n+1)\phi - \sum_{n=2}^{\infty}\left\{\sum_{k=1}^{\infty} (2k+n)\gamma_k\gamma_{k+n}\right\}\cos n\phi}{R\left[\left(1 + \sum_{k=1}^{\infty}\gamma_k^2\right) - \sum_{n=1}^{\infty} 2\gamma_n \cos(n+1)\phi + \sum_{n=2}^{\infty} 2\left(\sum_{k=1}^{\infty}\gamma_k\gamma_{k+n}\right)\cos n\phi\right]^{\frac{3}{2}}}. \tag{9}$$

One can now substitute (6) and (9) into the boundary condition (3) in order to determine the unknowns. It is better, however, to write (3) in the form $K = q^2 + \Gamma$, square both sides, cross-multiply, combine coefficients of the same harmonic and equate these coefficients to zero. We are then left with the following set of equations:

$$C_0^2 + \frac{1}{2}\sum_{k=2}^{\infty} C_k^2 = R^2\left[A_0 D_0 + \frac{1}{2}\sum_{k=2}^{\infty} A_k D_k\right], \quad \frac{1}{2}\sum_{k=0}^{n} C_k C_{n-k} + \sum_{k=0}^{\infty} C_k C_{k+n}$$

$$= \tfrac{1}{2}R^2\left[\sum_{k=0}^{n} A_k D_{n-k} + \sum_{k=0}^{\infty}(A_k D_{n+k} + A_{n+k} D_k)\right] \quad (n \geqslant 2), \tag{10}$$

where

$$A_0 = \left(1 + \sum_{k=1}^{\infty}\gamma_k^2\right), \quad A_n = 2\left(-\gamma_{n-1} + \sum_{k=1}^{\infty}\gamma_k\gamma_{k+n}\right) \quad (n \geqslant 2); \tag{11a}$$

$$B_0 = 2 + \Gamma A_0, \quad B_2 = -2 + \Gamma A_2, \quad B_n = \Gamma A_n \quad (n \geqslant 4); \tag{11b}$$

$$C_0 = 1 - \sum_{k=1}^{\infty} k\gamma_k^2, \quad C_n = (n-2)\gamma_{n-1} - \sum_{k=1}^{\infty}(2k+n)\gamma_k\gamma_{k+n} \quad (n \geqslant 2); \tag{11c}$$

$$D_0 = B_0^2 + \frac{1}{2}\sum_{k=2}^{\infty} B_k^2, \quad D_n = \frac{1}{2}\sum_{k=0}^{n} B_k B_{n-k} + \sum_{k=0}^{\infty} B_k B_{k+n} \quad (n \geqslant 2). \tag{11d}$$

Note that A_n, B_n, C_n and D_n vanish for odd n. The infinite system of equations above which needs to be solved for R, γ_1, γ_3, γ_5... is nonlinear and will, in general, have to be solved numerically. A great advantage is, however, immediately apparent: no field equations have to be solved and the equations are at most algebraic in the unknowns.

3. Analytical solutions

In this section we derive a number of analytical solutions to (10) for R and the coefficients $\gamma_1, \gamma_3, \gamma_5 \ldots$ in the mapping function $f(\zeta)$. These results are valuable not only because they help to better understand the nature of the solution and its dependence on the parameters of the problem, but also because they can be used as starting solutions for numerically solving the full system of nonlinear equations.

3.1. *Asymptotic solution for* $\Gamma \to \infty$

We know that when the bubble is stationary it is circular in section with radius $\hat{R}$ equal to $T/\Delta p$. If the bubble then moves slowly the shape will be approximately circular with the same radius; in this circumstance Γ will be very large since $\Gamma \approx 2\Delta p/\rho U^2$. We can, therefore, conclude that $R \sim \Gamma^{-1}$ and $\alpha_n \sim 0$ for $\Gamma \to \infty$. This suggests that we seek asymptotic expansions for the unknowns as $\Gamma \to \infty$ in the form

$$R^{-1} = \Gamma + r_0 + \Gamma^{-1} r_1 + \Gamma^{-2} r_2 + \ldots, \tag{12a}$$

$$\gamma_n = \Gamma^{-1} a_n + \Gamma^{-2} b_n + \ldots, \quad n = 1, 3, 5\ldots, \tag{12b}$$

Rather than work with (10) it is easiest to work directly with equations (6) and (9) for q^2 and K and the required boundary condition (3). Substituting the forms (12) into these three equations, expanding the terms for $\Gamma \to \infty$ and equating coefficients of the various powers of Γ^{-1} one can evaluate the unknowns in (12). The first correction to the reciprocal of the radius, r_0, turns out to be 2. Fortunately the only non-zero γ_n to order Γ^{-1} is γ_1; and subsequently only m of the γ_n turn out to be non-vanishing to order Γ^{-m}. Thus the solution to order Γ^{-2} is

$$R^{-1} = \Gamma + 2 + \tfrac{7}{9}\Gamma^{-1} + O(\Gamma^{-2}), \tag{13a}$$

$$\gamma_1 = -\tfrac{2}{3}\Gamma^{-1} + \tfrac{4}{9}\Gamma^{-2} + O(\Gamma^{-3}), \tag{13b}$$

$$\gamma_3 = -\tfrac{1}{15}\Gamma^{-2} + O(\Gamma^{-3}). \tag{13c}$$

As expected, for large Γ the bubble is approximately circular in section with a radius of Γ^{-1}. To the next approximation it appears (Shankar 1992) as an ellipse given by

$$x = (2+\Gamma)^{-1}(1 - \tfrac{2}{3}\Gamma^{-1})\cos\phi, \quad y = (2+\Gamma)^{-1}(1 + \tfrac{2}{3}\Gamma^{-1})\sin\phi \tag{14a, b}$$

Clearly the y-axis is the major axis, i.e. the bubble is flattened in the direction of flow. For smaller Γ there are, naturally, significant deviations from the elliptical section. In order to extend the range of validity of the asymptotic solutions we now determine it to higher order. To this end we assume asymptotic expansions for the relevant unknowns in the form

$$R^{-1} = \Gamma + r_0 + \Gamma^{-1} r_1 + \Gamma^{-2} r_2 + \Gamma^{-3} r_3 + \Gamma^{-4} r_4 + \ldots, \tag{15a}$$

$$\gamma_n = \Gamma^{-1} k_n + \Gamma^{-2} a_n + \Gamma^{-3} b_n + \Gamma^{-4} c_n + \Gamma^{-4} d_n + \ldots. \tag{15b}$$

Substituting (15) into (3) and collecting and equating to zero the coefficients of each harmonic of the azimuthal angle ϕ ($\phi = \arg(\zeta)$) one can determine the unknowns, viz. a_n, b_n, c_n, d_n etc. If this procedure had been attempted by hand it would have been formidable because of the complexity of the algebra involved. Now, however, using the symbolic manipulation program *Mathematica*, it has been possible to extend the expansion to order Γ^{-5}, leading to a representation accurate to very low values of Γ. We find that the unknown coefficients in (15) are given by

$$O(\Gamma^{-1}): \quad r_0 = 2, \quad k_1 = -\tfrac{2}{3}, \quad k_n = 0 \quad (n > 1); \tag{16a}$$

$$O(\Gamma^{-2}): \quad r_1 = \tfrac{7}{9}, \quad a_1 = \tfrac{4}{9}, \quad a_3 = -\tfrac{1}{15}, \quad a_n = 0 \quad (n > 3); \tag{16b}$$

$$O(\Gamma^{-3}): \quad r_2 = -\tfrac{10}{27}, \quad b_1 = -\tfrac{16}{135}, \quad b_3 = \tfrac{8}{225}, \quad b_5 = \tfrac{2}{189}, \quad b_n = 0 \quad (n > 5); \tag{16c}$$

$$O(\Gamma^{-4}): \quad r_3 = \tfrac{1}{2025}, \quad c_1 = -\tfrac{28}{225}, \quad c_3 = \tfrac{158}{2625}, \quad c_5 = -\tfrac{184}{6615}, \quad c_7 = -\tfrac{1}{675}, \quad c_n = 0 \quad (n > 7); \tag{16d}$$

$$O(\Gamma^{-5}): \quad r_4 = \tfrac{1568}{10125}, \quad d_1 = \tfrac{35482}{212625}, \quad d_3 = -\tfrac{304552}{2480625}, \quad d_5 = \tfrac{61912}{2083725}, \quad d_7 = \tfrac{4528}{637875}, \quad d_9 = \tfrac{2}{10395}. \tag{16e}$$

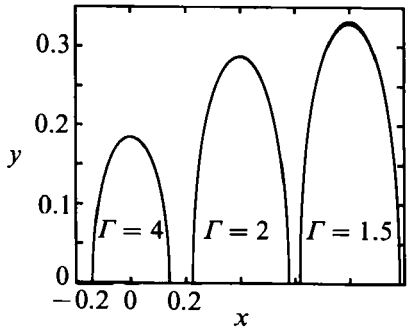

FIGURE 2. Comparison of bubble shapes as given by the asymptotic solution to order Γ^{-5} with the direct numerical solution. Note that to this scale the solutions overlap in the range considered.

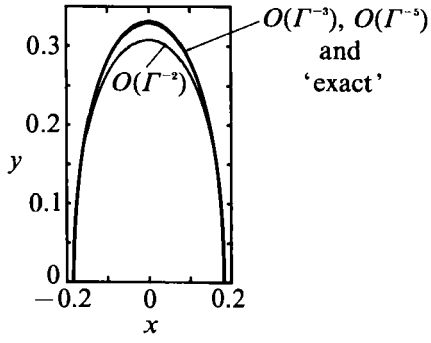

FIGURE 3. Comparison of the relative accuracies of the asymptotic solutions to various orders for large Γ. Solutions for $\Gamma = 1.5$.

The bubble shape then takes on the representation

$$x(\phi) = R[(-\tfrac{2}{3}\Gamma^{-1}+\tfrac{4}{9}\Gamma^{-2}+b_1\Gamma^{-3}+c_1\Gamma^{-4}+d_1\Gamma^{-5})\cos\phi+\tfrac{1}{3}(-\tfrac{1}{15}\Gamma^{-2}+b_3\Gamma^{-3}+c_3\Gamma^{-4}$$
$$+d_3\Gamma^{-5})\cos 3\phi+\tfrac{1}{5}(b_5\Gamma^{-3}+c_5\Gamma^{-4}+d_5\Gamma^{-5})\cos 5\phi$$
$$+\tfrac{1}{7}(c_7\Gamma^{-4}+d_7\Gamma^{-5})\cos 7\phi+\tfrac{1}{9}\Gamma^{-5}d_9\cos 9\phi]+O(\Gamma^{-6}), \tag{17a}$$

$$y(\phi) = R[(1+\tfrac{2}{3}\Gamma^{-1}-\tfrac{4}{9}\Gamma^{-2}-b_1\Gamma^{-3}-c_1\Gamma^{-4}-d_1\Gamma^{-5})\sin\phi-\tfrac{1}{3}(-\tfrac{1}{15}\Gamma^{-2}+b_9\Gamma^{-3}$$
$$+c_3\Gamma^{-4}+d_3\Gamma^{-5})\sin 3\phi-\tfrac{1}{5}(b_5\Gamma^{-3}+c_5\Gamma^{-4}+d_5\Gamma^{-5})\sin 5\phi$$
$$-\tfrac{1}{7}(c_7\Gamma^{-4}+d_7\Gamma^{-5})\sin 7\phi-\tfrac{1}{9}\Gamma^{-5}d_9\sin 9\phi]+O(\Gamma^{-6}), \tag{17b}$$

$$R = \Gamma+2+\tfrac{7}{9}\Gamma^{-1}-\tfrac{10}{27}\Gamma^{-2}+\tfrac{1}{2025}\Gamma^{-3}+r^4\Gamma^{-4}+O(\Gamma^{-5}). \tag{17c}$$

Note that, starting with $\exp(i\phi)$, each higher order picks up a succeeding harmonic; thus the structure of the solution remains very simple. In estimating the accuracy of any solutions obtained for the present problem a useful index is the maximum error in the satisfaction of the boundary condition (3) on the bubble surface; note that this is sufficient since the field equations and the conditions at infinity are automatically satisfied. Thus, henceforth the term 'error' will be used in this sense. An idea of the range of validity of the solution (17) derived for $\Gamma \to \infty$ can be gained from figures 2 and 3. Comparison with the direct numerical solutions show that the $O(\Gamma^{-5})$ solution is quite satisfactory for Γ as low as 2, when the error is approximately 0.0398; note that the error in the case of all direct numerical solutions

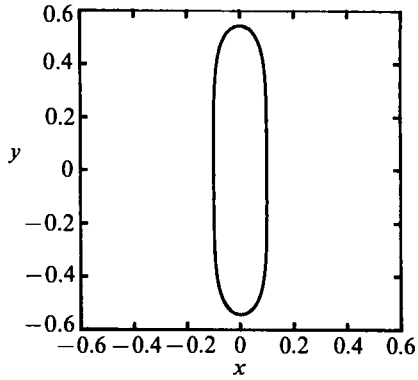

FIGURE 4. The shape of the bubble as given by the exact solution (19) for $\Gamma = 0$.

(sometimes to be called 'exact') is less than 10^{-10} and often less than 10^{-12}. When $\Gamma = 1.5$ the error is already as large as 0.213 but still the shape is well represented in figure 2. Figure 3 compares the shapes given by the lower-order solutions with the 'exact' solution for $\Gamma = 1.5$. It is seen that even the $O(\Gamma^{-3})$ solution is satisfactory for graphical accuracy.

3.2 *The exact solution for* $\Gamma = 0$

When the bubble excess pressure is exactly equal to the dynamic head, the parameter Γ takes the value zero. In this situation the boundary condition (3) implies a strict constraint on the bubble shape. For a symmetrical bubble stagnation points will occur on the x-axis. By (3) the curvature at these points has to equal Γ; thus the curvature on the axis is positive, zero or negative as Γ is positive, zero or negative. In particular the bubble has to be flat on the axis when Γ vanishes. One might thus hope for some simplification.

Equations (11) do simplify as the only non-zero B_n are B_0 and B_2, which take the values 2 and -2. Consequently the D_n simplify, the only non-vanishing ones being D_0, D_2 and D_4, which take the values 6, -8 and 2. Thus (11) simplifies considerably but still appears formidable. However, computations on the full equations for very small values of Γ suggest a very nice feature: that

$$R \to \tfrac{1}{3},\ \gamma_1 \to -\tfrac{2}{3},\ \gamma_3 \to -\tfrac{1}{9},\ \gamma_n \to 0\ (n \geqslant 5).$$

We are, therefore, led to the conjecture that for $\Gamma = 0$

$$R = \tfrac{1}{3},\ \gamma_1 = -\tfrac{2}{3},\ \gamma_3 = -\tfrac{1}{9},\ \gamma_n = 0 \quad (n \geqslant 5) \tag{18}$$

It is not difficult to show that (18) does indeed represent the exact solution to the infinite set of equations (11) for $\Gamma = 0$. The corresponding bubble shape is given parametrically by

$$x = \tfrac{1}{3}[\tfrac{1}{3}\cos\phi - \tfrac{1}{27}\cos 3\phi], \quad y = \tfrac{1}{3}[\tfrac{5}{3}\sin\phi + \tfrac{1}{27}\sin 3\phi]. \tag{19a,b}$$

When I first discovered this (Shankar 1992) I believed that it was the first exact solution for the shape of a translating bubble. However, a referee brought to my notice the fact that McLeod (1955) had discovered this solution almost 35 years earlier! His method, apparently devised for the case $\Gamma = 0$ alone, is quite different. The above exact solution is all the more remarkable in that it includes the effects of surface tension. The shape of the bubble is shown in figure 4; the bubble has an aspect ratio of $\frac{11}{2}$ and is flat on the x-axis as expected.

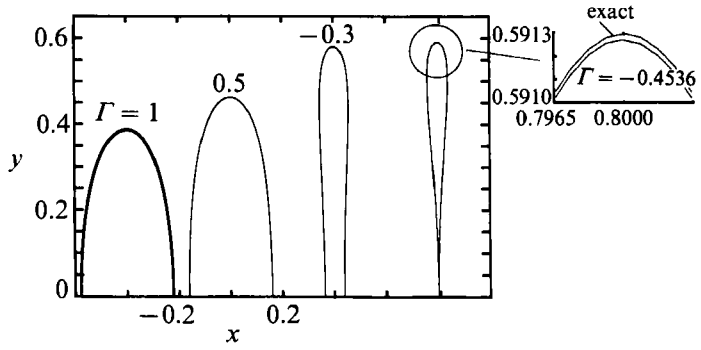

FIGURE 5. Bubble shapes given by the small-Γ solution correct to order Γ^6 compared with the 'exact' solution.

3.3. *An approximate solution for* $\Gamma \to 0$

With the exact solution for $\Gamma = 0$ to hand it is natural to seek a perturbation solution for $\Gamma \to 0$ around the known solution. To this end we assume the following forms for the unknowns as $\Gamma \to 0$:

$$R = r_0(1+\Gamma r_1+\Gamma^2 r_2+\ldots), \quad \gamma_1 = \gamma_{10}(1+\Gamma\alpha_1+\Gamma^2\beta_1+\ldots) \qquad (20a, b)$$

$$\gamma_3 = \gamma_{30}(1+\Gamma\alpha_3+\Gamma^2\beta_3+\ldots), \quad \gamma_n = \Gamma\alpha_n+\Gamma^2\beta_n+\ldots \quad (n \geqslant 5), \qquad (20c, d)$$

where $r_0 = \frac{1}{3}$, $\gamma_{10} = -\frac{2}{3}$ and $\gamma_{30} = -\frac{1}{9}$. These forms can now be substituted into the expressions (12) for A_n, B_n, C_n and D_n retaining terms till only the first order in Γ. These can then be substituted into (11) to obtain equations for the first corrections r_1 and α_n. Unfortunately this leads to an infinite system which is at least hexadiagonal. Instead, we obtain an approximate solution by truncating the system: retain only γ_1, γ_3, γ_5, γ_7 and γ_9, assume all other coefficients to vanish and solve only the first six equations for the six unknowns. In this manner we find the first six equations to be

$$\begin{bmatrix} -24184 & -45360 & 5022 & -65124 & -13122 & 0 & -39852 \\ 6940 & 2268 & 3726 & 45684 & 43254 & 8019 & -14256 \\ 6496 & 18576 & -3888 & 51192 & -39042 & -35964 & 7344 \\ 60 & -24 & 52 & 858 & 808 & -630 & -32 \\ 136 & 0 & 54 & -6156 & 11286 & 8856 & -108 \\ 4 & 0 & 0 & -486 & -2700 & 4950 & 0 \end{bmatrix} \begin{bmatrix} 1 \\ \alpha_1 \\ \alpha_3 \\ \alpha_5 \\ \alpha_7 \\ \alpha_9 \\ r_1 \end{bmatrix} = 0. \qquad (21)$$

This system of linear equations can be solved to yield

$$\alpha_1 = -\tfrac{19}{27}, \quad \alpha_3 = -\tfrac{44}{27}, \quad \alpha_5 = \tfrac{2}{243}, \quad \alpha_7 = \alpha_9 = 0, \quad r_1 = -\tfrac{2}{81}. \qquad (22)$$

Thus to first order in Γ we find the following approximate solution as $\Gamma \to 0$:

$$R = \tfrac{1}{3}(1-\tfrac{2}{81}\Gamma)+\ldots, \quad \gamma_1 = -\tfrac{2}{3}(1-\tfrac{19}{27}\Gamma)+\ldots, \qquad (23a\text{–}c)$$

$$\gamma_3 = -\tfrac{1}{9}(1-\tfrac{44}{27}\Gamma)+\ldots, \quad \gamma_5 = \tfrac{2}{243}\Gamma+\ldots, \quad \gamma_7 = O(\Gamma^{-2}), \quad \gamma_9 = O(\Gamma^{-2}). \qquad (23d\text{–}f)$$

Naturally this solution will not be accurate unless $|\Gamma| \ll 1$. In order to obtain a solution with a sufficiently large range of applicability we can extend the above

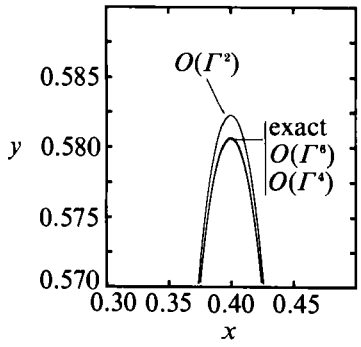

FIGURE 6. Small-Γ solution to various orders. Comparison with the exact solution for $\Gamma = -0.3$.

procedure to higher order. This has been carried out to order Γ^6; it is found that each order picks up only one extra harmonic without changing the lower-order terms.

Any doubts that one may have had over the value of the effort expended are likely to be dispelled by a glance at the results shown in figure 5. The perturbation solution obtained for $\Gamma \to 0$ gives very satisfactory bubble shapes from $\Gamma = 0.5$ (error $\approx$ 0.0043) down to $\Gamma = -0.4536$ (error ≈ -0.00025) close to pinch-off when the bubble ceases to be simply connected. Even for $\Gamma = 1.0$, when the error is large (≈ 0.328), the shape obtained is fair as figure 5 shows. It must be emphasized that an analytical representation has been obtained that not only has a large range of applicability but is capable of describing strongly necking bubbles which are notoriously difficult to compute directly.

Two parameters of geometrical interest are the bubble semi-major axis y_m and the bubble semi-minor axis x_m. In terms of the mapping coefficients they are given, to $O(\Gamma^6)$, by the formulae

$$x_m = R\left(1 + \sum_{n=1}^{15} \gamma_n/n\right), \tag{24a}$$

$$y_m = R\left(1 - \sum_{n=1}^{15} (-1)^{(n+3)/2}\gamma_n/n\right), \tag{24b}$$

with R and the γ_n evaluated from the higher-order solution. Note that to $O(\Gamma^n)$ these are nth-order polynomials in Γ. We remark that the solution of the polynomial equation $x_m = 0$ yields a value for the pinch-off value of Γ, Γ^*, when the opposite sides of the bubble touch. The sixth-order solution leads to a critical value of -0.4538, within 0.03% of the direct numerical estimate of -0.4537, while the fourth-order solution yields $\Gamma^* \approx -0.4525$.

In order to compare the accuracies likely to be obtainable using the solution for $\Gamma \to 0$ valid to different orders, we compare (figure 6) solutions correct to $O(\Gamma^2)$, $O(\Gamma^4)$ and $O(\Gamma^6)$ with the exact solution for $\Gamma = -0.3$. Even though the y-scale is greatly expanded the solutions merge except for the $O(\Gamma^2)$ solution; and even the latter is tolerable. In summary the $\Gamma \to 0$ solutions obtained here are accurate over a large range of Γ.

4. Numerical solutions and bubble parameters

Even a casual inspection of equations (10) will make obvious the need to seek numerical solutions if one desires great accuracy for arbitrary values of Γ. The iterative procedure that we have used is as follows. Newton's method is used to solve

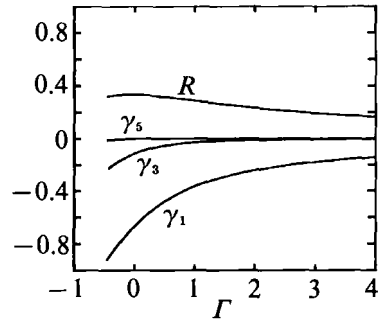

FIGURE 7. The variation of the coefficients in the mapping function with Γ.

	$\Gamma = -0.4$	$\Gamma = 1.0$	$\Gamma = 4.0$
R	0.324	0.287	0.162
γ_1	-0.886	-0.364	-0.141
γ_3	-0.215	-2.79×10^{-2}	-3.48×10^{-3}
γ_5	-8.78×10^{-3}	8.70×10^{-4}	8.41×10^{-5}
γ_7	-3.03×10^{-4}	-2.33×10^{-5}	-1.77×10^{-6}
γ_9	-9.63×10^{6}	5.76×10^{-7}	3.45×10^{-8}
γ_{11}	-2.91×10^{-7}	-1.35×10^{-8}	-6.39×10^{-10}
γ_{13}	-8.48×10^{-9}	3.07×10^{-10}	1.14×10^{-11}
γ_{15}	-2.42×10^{-10}	-6.81×10^{-12}	-2.00×10^{-13}
γ_{17}	-6.77×10^{-12}	1.48×10^{-13}	3.44×10^{-15}
γ_{19}	-1.95×10^{-13}	-3.19×10^{-15}	-5.85×10^{-17}

TABLE 1. R and the first ten significant coefficients for three values of Γ correct to 3 significant figures

the system of nonlinear equations, using the approximate solutions of the previous section as starting solutions. Assuming that the solution is known for $\Gamma = \Gamma_0$, change Γ be a small amount $\Delta\Gamma$. The expressions $\{e_{2k}(R, \gamma_1, \gamma_3, \ldots, \gamma_{2n-1}),\ k = 0, 1, 2, \ldots, n\}$ representing (11) will now not vanish. By making small changes $\Delta\gamma_k$ in turn, the terms of the generalized gradient $\partial e_l/\partial\gamma_k$ can be evaluated. One can then compute the corrections $\Delta\gamma_m$ needed to reduce the values of the e_j. Repeating the procedure one can converge to the solution for $\Gamma = \Gamma_0 + \Delta\Gamma$. This method did indeed work for all values of Γ even if the step size $\Delta\Gamma$ had at times to be made very small.

The general nature of how the first few γ_n and R vary with Γ is shown in figure 7. As shown in §3.1 all of these vanish as $\Gamma \to \infty$. R, γ_1 and γ_3 all increase in magnitude as $\Gamma \to 0$ until at $\Gamma = 0$ they take the values $\frac{1}{3}$, $-\frac{2}{3}$ and $-\frac{1}{9}$. At this point all the other coefficients vanish. As Γ decreases below 0 the magnitudes of R, γ_1 and γ_3 continue to increase, but now the other coefficients also become significant. Note that it is the decrease of γ_1 that is the principal cause of the necking of the bubble. Table 1 lists the first ten non-vanishing coefficients for three values of Γ.

Some bubble shapes for positive Γ are shown in figure 8. When $\Gamma = 8$ the bubble is almost circular in section but at $\Gamma = 4$ the deviations are already apparent. Initially both x_m and y_m, the minor and major axes, increase with Γ; but beyond $\Gamma \approx 1$, x_m decreases while y_m continues to increase. This can be seen quantitatively in figure 9. Comparison with the axisymmetric calculations of Miksis *et al.* (1981) shows that in general two-dimensional bubbles are much smaller than axisymmetric ones at the same value of Γ. Two other geometrical parameters of interest are the

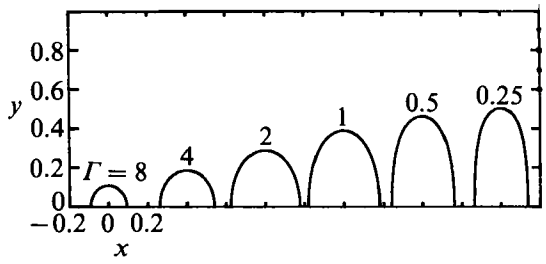

FIGURE 8. The shape of the bubble as Γ decreases. Only the upper half of the bubble is shown in each case.

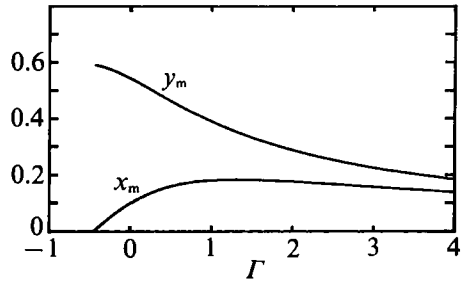

FIGURE 9. The dependence of x_m and y_m, the minor and major axes of the bubble, on Γ. The bubble ceases to be simply connected when $\Gamma \approx -0.4537$.

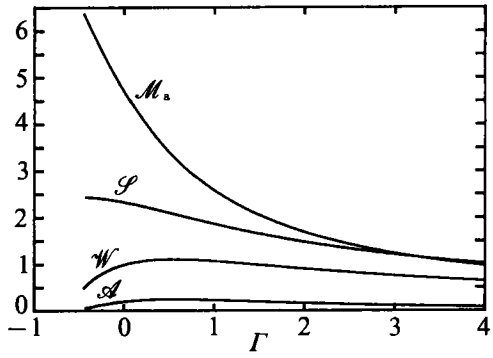

FIGURE 10. The variation of the bubble perimeter $\mathscr{S}$, area $\mathscr{A}$, Weber number $\mathscr{W}$, and added mass $\mathscr{M}_a$ with Γ.

perimeter $\mathscr{S}$ and the cross-sectional area $\mathscr{A}$; their dependence on Γ is indicated in figure 10.

Two quantities of dynamical interest are the Weber number $\mathscr{W}$ and the added mass $\mathscr{M}_a$. Once the area $\mathscr{A}$ is computed the Weber number can be computed from the formula

$$\mathscr{W} = \rho U^2(\mathscr{A}/\pi)^{\frac{1}{2}}/T = 4(\mathscr{A}/\pi)^{\frac{1}{2}}. \tag{25}$$

For the added mass we refer to Milne–Thompson (1960, pp. 238, 240). Thus, in his notation, when the potential Φ has, for $r \to \infty$, the expansion

$$\Phi = Ux + Ax/r^2 + By/r^2 + \ldots, \tag{26}$$

the added mass $\hat{\mathscr{M}}_a$ is given by

$$\hat{\mathscr{M}}_a = (2\pi A - VU)\rho/U, \tag{27}$$

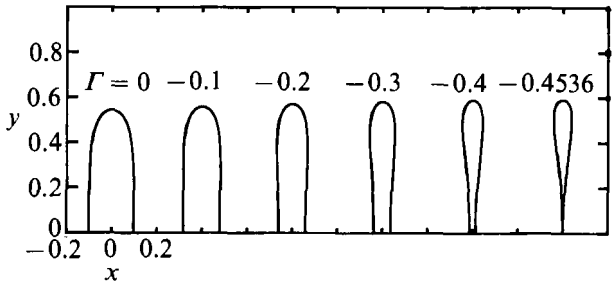

FIGURE 11. Non-convex bubble shapes for negative Γ.

and so for our bubble motion the dimensionless added mass in our notation is given by

$$\mathscr{M}_a = 2\pi(R^2 - a_1) - \mathscr{A}. \tag{28}$$

The dependence of the Weber number and added mass on Γ is shown in figure 10. As in the axisymmetric case and as conjectured in Shankar (1991) there is a maximum Weber number above which no steady solution exists. This maximum is approximately 1.11, as opposed to 3.23 in the axisymmetric case. The added mass has to vanish as $\Gamma \to \infty$ since a circular section has zero added mass. As Γ decreases, the increasing distortion of the bubble in the y-direction causes $\mathscr{M}_a$ to increases rapidly.

Our experience has been that it is very easy to compute to great accuracy for $\Gamma > 0$. But when the parameter becomes negative the computations become increasingly difficult. It appears that this problem is a general one. Miksis *et al.* clearly indicate their difficulties in this region and stop their computations well short of the minimum possible Γ corresponding to pinch-off; moreover, their bubble shapes show fore–aft asymmetry. Meiron (1989) does not display any bubble shapes which clearly show necking. With the method adopted here it was possible to compute accurately down to pinch-off but the step size $\Delta\Gamma$ had at times to be reduced to 10^{-4}. Figure 11 shows the non-convex bubble shapes that develop for negative Γ. While the major axis of the bubble changes little, necking causes the minor axis to reduce monotonically until the sides of the bubble touch; the value of Γ at pinch-off (Γ^*) is approximately -0.4537; beyond this value the bubble can no longer be simply connected. The corresponding value in the axisymmetric case has been estimated by Miksis *et al.* to be about -0.31; their estimate was based on an extrapolation from computations done up to $\Gamma = -0.251$.

5. Discussion and conclusion

Our aim was to obtain analytical descriptions of the bubble shape over as large a range of Γ-values as possible. The results of §3.1 cover the range $2 \leqslant \Gamma < \infty$, corresponding to comparatively slow to moderately fast bubble speeds. The results obtained in §3.3 give bubble shapes in the range $-0.4537 < \Gamma \leqslant 0.75$, for very rapidly moving bubbles down to the condition where the necking bubble ceases to exist as a single entity. With some sacrifice in accuracy the results can be used in the extended ranges $\Gamma \leqslant 1.0$ and $\Gamma \geqslant 1.5$. It is somewhat surprising, but gratifying, that the asymptotic expansions of extremely simple form derived here cover almost the entire range of possible Γ-values.

A summary of the range covered by the present results is contained in figure 12.

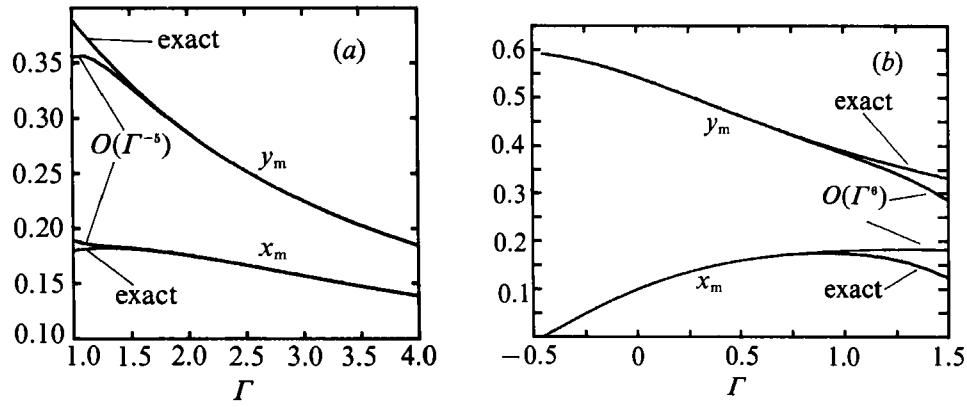

FIGURE 12. (*a*) The dimensions of the semi-major and semi-minor axes of the bubble as given by the large-Γ solution to order Γ^{-5}: (*b*) Comparison of the semi-major and semi-minor axes of the bubble as given by the small-Γ solution with those of the exact solution.

Figure 12(a) shows the dimensions of the semi-major axis y_m and the semi-minor axis x_m of the bubble as a function of Γ for $\Gamma \to \infty$. The corresponding results for $\Gamma \to 0$ are shown in figure 12(*b*). While the range covered by the two solutions is very great it may be noted that neither picks up the maximum value of x_m around $\Gamma \approx 1.3$. Possibly, taking even higher-order terms in each expansion would lead to greater ranges of validity, sufficient to pick up the maximum.

We wish to remark on an issue that is relevant to direct numerical computation. With the analytical approach used here it was possible to estimate the 'error' in the computed solutions. A feature that was noted and has been indicated above is that even with comparatively large errors on the boundary the bubble shape tends to appear reasonable. Conversely, it is likely that a reasonable looking bubble can have large errors associated with it. This is particularly serious for direct numerical computations. Thus in Miksis *et al.* (1981) the bubble shapes shown in their figure 2 show slight fore–aft asymmetry; if these are not due to graphing errors the associated solutions are not likely to be accurate.

The asymptotic solutions obtained here should be useful in any viscous analysis of two-dimensional bubble shapes. Note in particular that a good description of necking bubbles has been obtained for $\Gamma < 0$, a facility still not available in the axisymmetric case. The asymptotic results can also be used for approximate, quasi-steady computations of unsteady bubble motions. Once again it is the simplicity of the analytical description that should be of help.

We conclude by emphasizing that the present asymptotic results eliminate the need for direct numerical computations over a large range of Γ unless extremely great accuracy is required. The large-Γ solution was possible because it was known that the bubble had to be approximately circular in section when it was slow moving. The solution for small Γ became feasible once the exact solution for $\Gamma = 0$ was rediscovered. Of particular interest are the solutions in the range $\Gamma < 0$, when the bubble begins to neck. It is remarkable that the $O(\Gamma^6)$ solution is able to give such a good estimate of the pinch-off value of Γ, $\Gamma^* \approx 0.4537$, when the bubble ceases to be simply connected. This range of Γ, $\Gamma < 0$, is very difficult to compute. In fact, in the axisymmetric case, the value of $\Gamma^*(\approx -0.31)$ has been found only by extrapolation. Thus it may not be an extravagant claim that the conformal mapping technique and the resulting exact and asymptotic solutions have led to a rich bounty of valuable and useful results in bubble dynamics.

I would like to thank Uday Sinha and the Flosolver group for having made *Mathematica* available to me. My thanks also go to a referee for bringing McLeod's work to my notice, and to C. N. Ravi for help in preparing the manuscript.

REFERENCES

BAKER, G. R. & MOORE, D. W. 1989 The rise and distortion of a two-dimensional gas bubble in an inviscid liquid. *Phys. Fluids* A **1**, 1451.

BENJAMIN, T. B. 1987 Hamiltonian theory for motions of bubbles in an infinite liquid. *J. Fluid Mech.* **181**, 349.

LUNDGREN, T. S. & MANSOUR, N. N. 1991 Vortex ring bubbles. *J. Fluid Mech.* **224**, 177.

MCLEOD, E. B. 1955 The explicit solution of a free boundary problem involving surface tension. *J. Rat. Mech. Anal.* **4**, 557.

MEIRON, D. I. 1989 On the stability of gas bubbles rising in an inviscid fluid. *J. Fluid Mech.* **198**, 101.

MIKSIS, M., VANDEN-BROECK, J. M. & KELLER, J. B. 1981 Axisymmetric bubbles or drops in a uniform flow. *J. Fluid Mech.* **108**, 89.

MILNE-THOMPSON, L. M. 1960 *Theoretical Hydrodynamics*, 4th Edn. Macmillan.

MOORE, D. W. 1959 The rise of a gas bubble in a viscous liquid, *J. Fluid Mech.* **6**, 113.

MOORE, D. W. 1965 The velocity of rise of distorted gas bubbles in a liquid of small viscosity. *J. Fluid Mech.* **23**, 749.

SHANKAR, P. N. 1991 Exact solutions for a class of non-linear free surface flows. *Proc. R. Soc. Lond.* A **434**, 677.

SHANKAR, P. N. 1992 Two-dimensional bubbles in uniform motion. *N.A.L. document* PD CF 9201.

WALTERS, J. K. & DAVIDSON, J. F. 1962 The initial motion of a gas bubble formed in an inviscid liquid. Part 1. The two-dimensional bubble. *J. Fluid Mech.* **12**, 408.